

Side chain contributions to the interconversion of the topological isomers of guanylin-like peptides

AXEL SCHULZ,^{a*} UTE C. MARX,^b NAOMI TIDTEN,^b THOMAS LAUBER,^b YUJI HIDAKA^c and KNUT ADERMANN^a

^a IPF PharmaCeuticals GmbH, Feodor-Lynen-Strasse 31, D-30625 Hannover, Germany

^b Lehrstuhl für Struktur und Chemie der Biopolymere, Universität Bayreuth, D-95447 Bayreuth, Germany

^c Department of Life Science, Faculty of Science and Engineering, Kinki University, Higashi-Osaka, Osaka 577-8502, Japan

Received 8 July 2004; Accepted 12 August 2004

Abstract: The peptide hormones guanylin and uroguanylin are ligands of the intestinal guanylyl cyclase-C (GC-C) that is involved in the regulation of epithelial water and electrolyte transport. The small peptides contain 15 and 16 amino acids, respectively, and two disulfide bonds with a 1–3/2–4 connectivity. This structural feature causes the unique existence of two topological isoforms for each peptide in an approximate 3:2 ratio, with only one of the isoforms exhibiting GC-C-activating potential. The two uroguanylin isomers can be separated by HPLC and are of sufficient stability to be studied separately at ambient temperatures while the two guanylin isomers are rapidly interconverting even at low temperatures. Both isomers show clearly distinguishable ¹H chemical shifts. To investigate the influence of certain amino acid side chains on this isomerism and interconversion kinetics, derivatives of guanylin and uroguanylin (L-alanine scan and chimeric peptides) were designed and synthesized by Fmoc solid-phase chemistry and compared by HPLC and 2D ¹H NMR spectroscopy. Amino acid residues with the most significant effects on the interconversion kinetics were predominantly identified in the COOH-terminal part of both peptides, whereas amino acids in the central part of the peptides only moderately affected the interconversion. Thus, the conformational conversion among the isomers of both peptides is under the control of a COOH-terminal sterical hindrance, providing a detailed model for this dynamic isomerism. Our results demonstrate that kinetic control of the interconversion process can be achieved by the introduction of side chains with a defined sterical profile at suitable sequence positions. This is of potential impact for the future development of GC-C peptide agonists and antagonists. Copyright © 2004 European Peptide Society and John Wiley & Sons, Ltd.

Keywords: guanylin; uroguanylin; topological isomers; interconversion; NMR spectroscopy

INTRODUCTION

Guanylin and uroguanylin are small mammalian peptide hormones that stimulate chloride secretion via the activation of transmembrane guanylyl cyclase-C (GC-C) [1–3]. The two peptide hormones of 15 and 16 amino acid residues, respectively, are characterized by two disulfide bonds with a 1–3/2–4 cysteine pattern which is crucial for biological activity [1]. Due to the two disulfides located within a short stretch of 12 amino acids (Figure 1), both guanylin and uroguanylin show a unique topological stereoisomerism which is detectable using NMR spectroscopy and temperature-dependent HPLC [4–6]. Both peptides form two topological isomers in an approximately 3:2 ratio in solution, but only the preferred and earlier eluting isomer, referred to

as isomer A, activates GC-C [6,7]. While the two isoforms of guanylin interconvert with a half-life of seconds and are only detectable at low temperatures during HPLC analysis [4], the interconversion of the topological isomers of uroguanylin is significantly slower and the two isoforms can be separated by HPLC (Figure 2) [6,8,9]. The different interconversion kinetics of uroguanylin isomers has been attributed to the COOH-terminal leucine residue which is absent in guanylin. A uroguanylin derivative lacking this amino acid exhibits similar HPLC characteristics to guanylin [8]. Correspondingly, a guanylin derivative COOH-terminally extended by leucine shows interconversion kinetics similar to that of uroguanylin, and thus the two corresponding isomers are separable [7]. The solution structures of guanylin and uroguanylin determined by NMR spectroscopy show two distinct stereoisomers for each peptide, termed A- and B-isoforms, which can be distinguished easily by their typical backbone ¹H chemical shifts [5,6]. Only the respective structure of the A-isoform of either peptide closely resembles the structure of *Escherichia coli* heat-stable enterotoxin ST which is a strong agonist of GC-C [6,7,10]. ST contains a third disulfide bond that is responsible for its conformational rigidity and the lack of topological isomers [11].

Abbreviations: Acn, acetamidomethyl; ESI-MS, electrospray ionization mass spectrometry; Fmoc, 9-fluorenylmethoxycarbonyl; GC-C, guanylyl cyclase-C; HBTU, 2-(1H-benzotriazol-1-yl)-N,N,N',N'-bis(tetramethylene)uronium hexafluorophosphate; NMR spectroscopy, nuclear magnetic resonance spectroscopy; NOESY, nuclear Overhauser enhancement spectroscopy; RP-HPLC, reversed phase high performance liquid chromatography; ST, *Escherichia coli* heat-stable enterotoxin; TFA, trifluoroacetic acid; TOCSY, total correlation spectroscopy; Trt, trityl.

*Correspondence to: Dr Axel Schulz, IPF PharmaCeuticals GmbH, Feodor-Lynen-Strasse 31, D-30625 Hannover, Germany; e-mail: a.schulz@ipf-pharmaceuticals.de

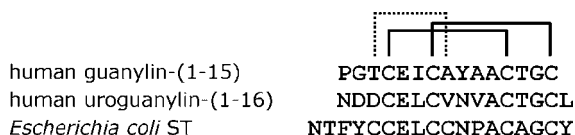


Figure 1 Amino acid sequences of GC-C-activating peptides guanylin, uroguanylin and *Escherichia coli* heat-stable enterotoxin ST. Disulfide bridges are indicated. The dotted disulfide bond corresponds to the additional disulfide of ST.

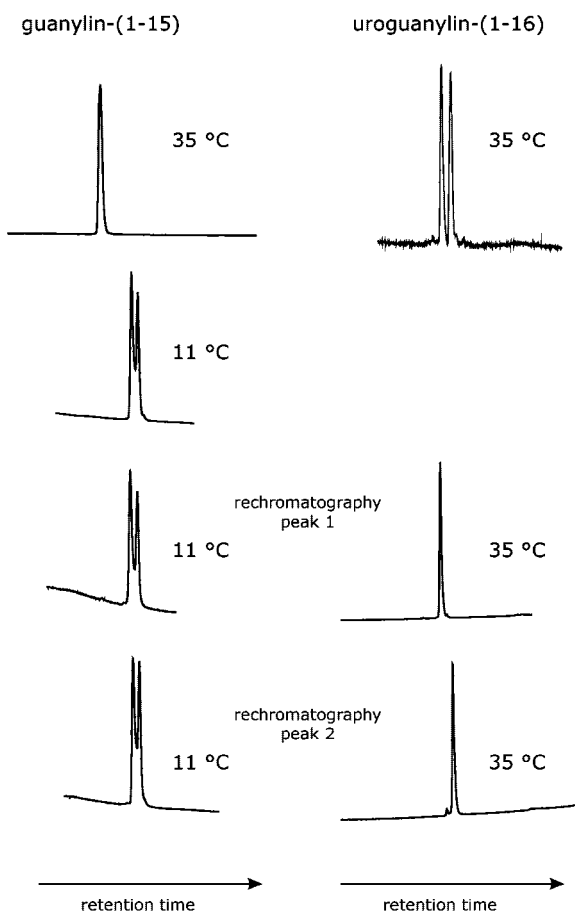


Figure 2 Analytical HPLC profiles of guanylin-(1-15) **1** and uroguanylin-(1-16) **13** at different column temperatures. The peaks appearing in the chromatograms were collected and analysed under the same conditions.

The biological importance of guanylin and uroguanylin and their transmembrane guanylyl cyclase-C receptor is reflected by the fact that infection with enterotoxigenic strains of *E. coli* secreting the agonistic and highly potent heat-stable enterotoxin ST is a main cause of infant mortality in developing countries and of traveler's diarrhea [12–14]. Novel findings using uroguanylin-deficient mice suggest a role for uroguanylin in the enteric–renal communication axis, linking the intestine and kidney in an endocrine way for the maintenance of sodium balance [15]. Furthermore, uroguanylin was shown to induce apoptosis in human colon carcinoma cells *in vitro*. It may, therefore, have a therapeutic

potential for the prevention or treatment of colon cancer [16].

Structural heterogeneity due to topological stereoisomerism is known for a few other small cysteine-rich peptides such as the conotoxins, peptide neurotoxins produced by *Conus* snails. Using NMR spectroscopy, α -conotoxins show one major species (over 80%) and multiple minor conformations, but structure determination was only possible for the major isoform [17,18]. The conotoxin sequences from different species contain, however, at least one proline or hydroxyproline residue that might contribute to the structural heterogeneity. Such *cis/trans* isomerism at a hydroxyproline peptide bond has been found for a μ -conotoxin [19]. Contryphans, another family of small peptides isolated from *Conus* snails containing a D-amino acid, one disulfide bond and a hydroxyproline and/or proline residue, also exhibit two distinct interconvertible conformational states, as detected by HPLC methods [20,21]. NMR-spectroscopic structure determination revealed that the two distinct structural states are due to *cis/trans* isomerism of the cysteine-hydroxyproline peptide bond, with the major conformer exhibiting *cis* orientation [22,23]. To our knowledge, guanylin and uroguanylin are the only known peptides exhibiting topological isomerism without the presence of a proline or hydroxyproline residue. It has been shown previously that the interconversion of guanylin and uroguanylin isomers is independent of the peptide concentration, and no indications for an opening and rearrangement of the disulfide bonds during the interconversion were found [4,6].

In this study, a set of L-alanine-substituted peptides (L-alanine scan) and chimeric peptides of guanylin, uroguanylin and *E. coli* ST were designed, synthesized and investigated using temperature-dependent HPLC analysis and NMR spectroscopy in order to determine the amino acid residues influencing the interconversion of guanylin and uroguanylin peptides, and thereby substantiating and refining the mechanism for this unique type of conformational isomerism.

MATERIALS AND METHODS

Peptide Synthesis

Guanylin peptides (Table 1) were synthesized on a preloaded TentaGel-S-PHB Fmoc-Cys(Acm) resin (Rapp Polymere, Tübingen, Germany). Uroguanylin peptides (Table 2) were synthesized on a preloaded H-Leu-2-CI-Trt resin (Novabiochem, Bad Soden, Germany) except for [Ala¹⁶]-uroguanylin **14** which was synthesized on a preloaded H-Ala-2-CI-Trt resin (Novabiochem, Bad Soden, Germany). Acylations were carried out using HBTU activation on a 433 A peptide synthesizer (Applied Biosystems, Weiterstadt, Germany) applying standard Fmoc chemistry. For selective introduction of disulfide bonds, Cys⁷ and Cys¹⁵ were Acm-protected, while Cys⁴ and Cys¹² were Trt-protected. Disulfides were subsequently introduced by air

Table 1 Sequences of Guanylin L-Alanine Peptides Used in this Study

No.	Peptide	Sequence
1	Guanylin-(1–15)	PGTCEICAYA AACTGC
2	[Ala ¹⁴]-guanylin-(1–15)	PGTCEICAYA AACT A C
3	[Ala ¹³]-guanylin-(1–15)	PGTCEICAYA A A CAGC
4	[Ala ⁹]-guanylin-(1–15)	PGTCEICA A AACTGC
5	[Ala ⁶]-guanylin-(1–15)	PGTCE A CAYA AACTGC
6	[Ala ⁵]-guanylin-(1–15)	PGTCA A ICAYA AACTGC
7	[Ala ³]-guanylin-(1–15)	PG A CEICAYA AACTGC
8	[Ala ²]-guanylin-(1–15)	PA T CEICAYA AACTGC
9	[Ala ¹]-guanylin-(1–15)	A GTCEICAYA AACTGC
10	des-Gly ² -guanylin-(1–15)	P.TCEICAYA AACTGC
11	[Val ⁸ , Asn ⁹ , Val ¹⁰]-guanylin-(1–15)	PGTCEIC VNV ACTGC
12	[Asn ⁹ , Pro ¹⁰]-guanylin-(1–15)	PGTCEICAN P ACTGC

The disulfide bonds are indicated. Mutated residues are shown in bold.

oxidation and iodine treatment. For a detailed description of the synthetic procedure, see Klodt *et al.* [4]. Peptide purity was checked by RP-HPLC (Vydac C18, The Separations Group, Hesperia, USA) and ESI-MS (Perkin Elmer, Sciex API 100, Foster City, USA). Stereoisomers of uroguanylin peptides were separated by RP-HPLC on a Vydac C18 column (5 μ m, 300 \AA , 20 \times 250 mm, 8 ml/min, detection at 215 nm; eluent A: 0.1% TFA, eluent B: 0.07% TFA in acetonitrile/water 4:1; gradient 20%–50% eluent B in 60 min, or a pH 7 eluent system with eluent A: 20 mM phosphate buffer, pH 7, eluent B: 20 mM phosphate/acetonitrile 2:3; gradient 10%–40% eluent B in 60 min; for peptides **14**, **16**, **19** (Table 2)).

Analytical High Performance Liquid Chromatography

The interconversion of guanylin and uroguanylin peptides was investigated on a Nucleosil C18 PPN column (Macherey & Nagel, Düren, Germany, 5 μ m, 100 \AA , 2 \times 250 mm, 0.2 ml/min, UV detection at 215 nm) using either eluent system 1 (eluent A: 0.1% TFA, eluent B: 0.07% TFA in acetonitrile/water 4:1) or eluent system 2 (eluent A: 10 mM NH₄OAc, pH 5.7, eluent B: 10 mM NH₄OAc/acetonitrile 1:4) at column temperatures of 11 $^{\circ}$ C, 35 $^{\circ}$ C and 50 $^{\circ}$ C for guanylin peptides and column temperatures of 25 $^{\circ}$ C and 35 $^{\circ}$ C for uroguanylin peptides.

Interconversion Studies of Guanylin Peptides

For the interconversion studies of guanylin analogs, the peptides were loaded onto an analytical HPLC column and a gradient of 10%–70% eluent B (eluent system 1) in 60 min at a flow rate of 0.2 ml/min was applied. The appearing peaks were separated, immediately frozen in liquid nitrogen, lyophilized, reconstituted in water and loaded directly onto the same HPLC column for repeated chromatographic separation at 11 $^{\circ}$ C.

Interconversion Studies of Uroguanylin Peptides

For the interconversion of uroguanylin peptides, the separated forms of each analog were dissolved in water (pH 4.5) at a concentration of 1 μ g/ μ l and incubated at 37 $^{\circ}$ C. After 3, 6, 24, 48, 72 and 168 h, samples of 10 μ l were taken and lyophilized. The samples were then stored at –20 $^{\circ}$ C prior to analytical HPLC (eluent system 2, 10%–70% B in 60 min). The peak areas detected were integrated using the Kroma System 2000 software (Kontron, Neufahrn, Germany). The percentage of peak 1 was plotted against the incubation time and then analysed using a first order exponential fit function (Graph Pad Prism, San Diego, USA).

NMR Spectroscopy

Two-dimensional NMR spectra were recorded on a Bruker DRX 600 MHz or Bruker AVANCE 400 MHz spectrometer (Bruker, Karlsruhe, Germany) at 11 $^{\circ}$ C. The peptide concentrations ranged from 0.4 to 1.2 mM in aqueous solution, pH 3.6–3.9 in H₂O/D₂O (9:1, v/v, 500 μ l). Water suppression was performed by excitation sculpting for NOESY and the z-filtered TOCSY spectra [24,25]. The spectra were recorded with a spectral width of 6613.8 Hz in both dimensions and 4 K \times 0.5 K data points in the time domain. Quadrature detection was used in both dimensions with the time proportional phase incrementation technique in ω_1 . Spectra were multiplied with a squared Sinebell function phase shifted by $\pi/4$ for the NOESY (mixing time 200 ms), and the z-filtered TOCSY (mixing time 80 ms) prior to Fourier transformation. Application of zero filling resulted in 4 K \times 1 K data points in the frequency domain. Baseline correction was achieved using a model-free algorithm [26]. Data were evaluated on X-window workstations with the NDee program package (SpinUp, Dortmund, Germany).

RESULTS

Interconversion of Guanylin Peptides

To gain insight into the interconversion kinetics of guanylin peptides, native guanylin **1**, eight side chain-substituted alanine mutants (peptides **2–9**, Table 1), a deletion mutant lacking Gly², and chimeric peptides of guanylin, uroguanylin and ST (peptides **10–12**) were synthesized and subjected to HPLC analysis under different elution conditions and separation temperatures. At a high temperature of 50 $^{\circ}$ C, all synthetic peptides exhibited only one peak during HPLC analysis using the standard eluent system at pH 2. At a lower column temperature of 11 $^{\circ}$ C, the native guanylin peptide **1** showed two different isoforms that were interconverting within approximately 30 min, the time required for rechromatography of the separated peaks (Figure 2) [4]. The HPLC profile of peptides that exhibited a notably different behavior compared with native guanylin **1** using the standard eluent system are shown in Figure 3. The substitution of Gly¹⁴ by Ala in peptide **2** (Figure 3A) caused a significant reduction in the interconversion rate, generating two

Table 2 Sequences and Half-life Constants of Uroguanylin L-Alanine Peptides Used in this Study

No.	Peptide	Sequence	$t_{1/2}$ (min) ^a	
			A	B
13	Uroguanylin-(1–16)	NDDCELCVNVACTGCL	1055	898
14	[Ala ¹⁶]-uroguanylin-(1–16)	NDDCELCVNVACTG C A	41	53
15	[Ala ¹⁴]-uroguanylin-(1–16)	NDDCELCVNVACT A CL	n.d. ^b	n.d. ^b
16	[Ala ¹³]-uroguanylin-(1–16)	NDDCELCVNVAC A GCL	947	1137
17	[Ala ¹⁰]-uroguanylin-(1–16)	NDDCELCV N A A CTGCL	891	1164
18	[Ala ⁹]-uroguanylin-(1–16)	NDDCELCV A VACTGCL	395	173
19	[Ala ⁸]-uroguanylin-(1–16)	NDDCELC A NVACTGCL	581	2130
20	[Ala ⁶]-uroguanylin-(1–16)	NDDCE A CVNVACTGCL	2529	817
21	[Ala ⁵]-uroguanylin-(1–16)	NDD C ALCVNVACTGCL	1356	1148
22	[Ala ³]-uroguanylin-(1–16)	N D ACELCVNVACTGCL	470	1064
23	[Ala ²]-uroguanylin-(1–16)	N A DCELCVNVACTGCL	1664	379
24	[Ala ¹]-uroguanylin-(1–16)	A DDCELCVNVACTGCL	969	723
25	[Ala ⁸ , Tyr ⁹ , Ala ¹⁰]-uroguanylin-(1–16)	NDDCELC A Y A ACTGCL	457	382
26	[Pro ¹⁰]-uroguanylin-(1–16)	NDDCELCV N PACTGCL	1953	1631

The disulfide bonds are indicated. Mutated residues are shown in bold.

^a $t_{1/2}$ was calculated using a first order exponential fit function (Graph Pad Prism).

^b n.d. = not determined.

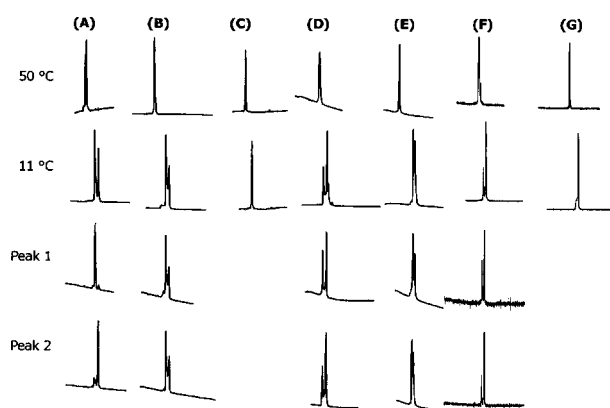


Figure 3 Analytical HPLC profiles of guanylin derivatives at different column temperatures and rechromatography of the separated isomers. (A) [Ala¹⁴]-guanylin-(1–15) **2**, (B) [Ala¹³]-guanylin-(1–15) **3**, (C) [Ala⁹]-guanylin-(1–15) **4**, (D) [Ala⁶]-guanylin-(1–15) **5**, (E) [Ala⁵]-guanylin-(1–15) **6**, (F) [Asn⁹, Pro¹⁰]-guanylin-(1–15) **12**, (G) [Val⁸, Asn⁹, Val¹⁰]-guanylin-(1–15) **11**.

permanently separable isoforms similar to uroguanylin isoforms (Figure 2). The mutation in [Ala¹³]-guanylin (**3**, Figure 3B) caused a slightly faster interconversion and it was not possible to accumulate either isomer by HPLC. Chromatographic analysis of [Ala⁹]-guanylin (**4**, Figure 3C) showed only one peak at 11 °C. Using 2D NMR spectroscopy, two different sets of spin systems with chemical shifts similar to those of the isoforms of native guanylin **1** were identified, revealing the existence of the typical two isoforms. The HPLC pattern

of [Ala⁶]-guanylin (**5**, Figure 3D) revealed a ratio of the two isoforms that differs from the 3:2 ratio found for native guanylin **1** with the later eluting isomer being present in a higher population. [Ala⁵]-guanylin (**6**, Figure 3E) exhibited a faster interconversion than native guanylin **1**. Peptides **7** to **9** with mutations at the NH₂-terminus showed no notable difference in their HPLC patterns from that of **1**. The deletion peptide **10** lacking Gly² which has a short NH₂-terminus of two amino acid residues displayed only one HPLC peak at a separation temperature of 11 °C similar to peptide **4**. Using a different eluent system at pH 5.7, peptide **10** showed two distinct peaks at 11 °C (data not shown). A chimeric peptide of guanylin and uroguanylin (**11**, Figure 3G) exhibited one peak with a front shoulder during HPLC analysis at 11 °C, while the hybrid derivative of guanylin and ST (**12**, Figure 3F) showed two separate but interconverting peaks in a ratio of about 2:3. In summary, only the isoforms of [Ala¹⁴]-guanylin **2** revealed a decreased interconversion rate compared with native guanylin, strongly suggesting the participation of the COOH-terminal amino acid side chains in the interconversion.

Interconversion of Uroguanylin Peptides

In contrast to the guanylin derivatives, all L-alanine mutant peptides derived from native uroguanylin (**13**, Table 2) existed as two separable isoforms, allowing a more detailed analysis of the interconversion. In the following, the earlier eluting isomer of the uroguanylin

derivatives is referred to as isomer A, and the more retarded component as isomer B. The separated isomers were incubated in aqueous solution at 37 °C (pH 4.5). Samples were taken after 3, 6, 24, 48, 72 and 168 h and analysed using HPLC and ESI-MS. An NH₄OAc eluent system at pH 5.7 was applied for HPLC analysis of the samples because the isomers of all uroguanylin derivatives were detectable using these conditions. The ratio of isomers was calculated by HPLC peak integration. To illustrate the mutual interconversion of the isoforms of selected derivatives, the percentage of isomer A was plotted against

the incubation time (Figure 4). The most striking alterations in the interconversion kinetics compared with native uroguanylin (**13**, Figure 4A) were found for peptides **14** and **15** (Figure 4B, C). The interconversion of the [Ala¹⁶]-uroguanylin mutant **14** was significantly accelerated, reflected by a steeper slope of both curves. The equilibrium between the isomers was reached after 6 h. The exchange of Gly¹⁴ by Ala in peptide **15** led to a significant deceleration of the interconversion. The isomerization of **15** did not reach an equilibrium after 7 days of incubation, although the interconversion from the A-form to the B-form appeared to be slightly

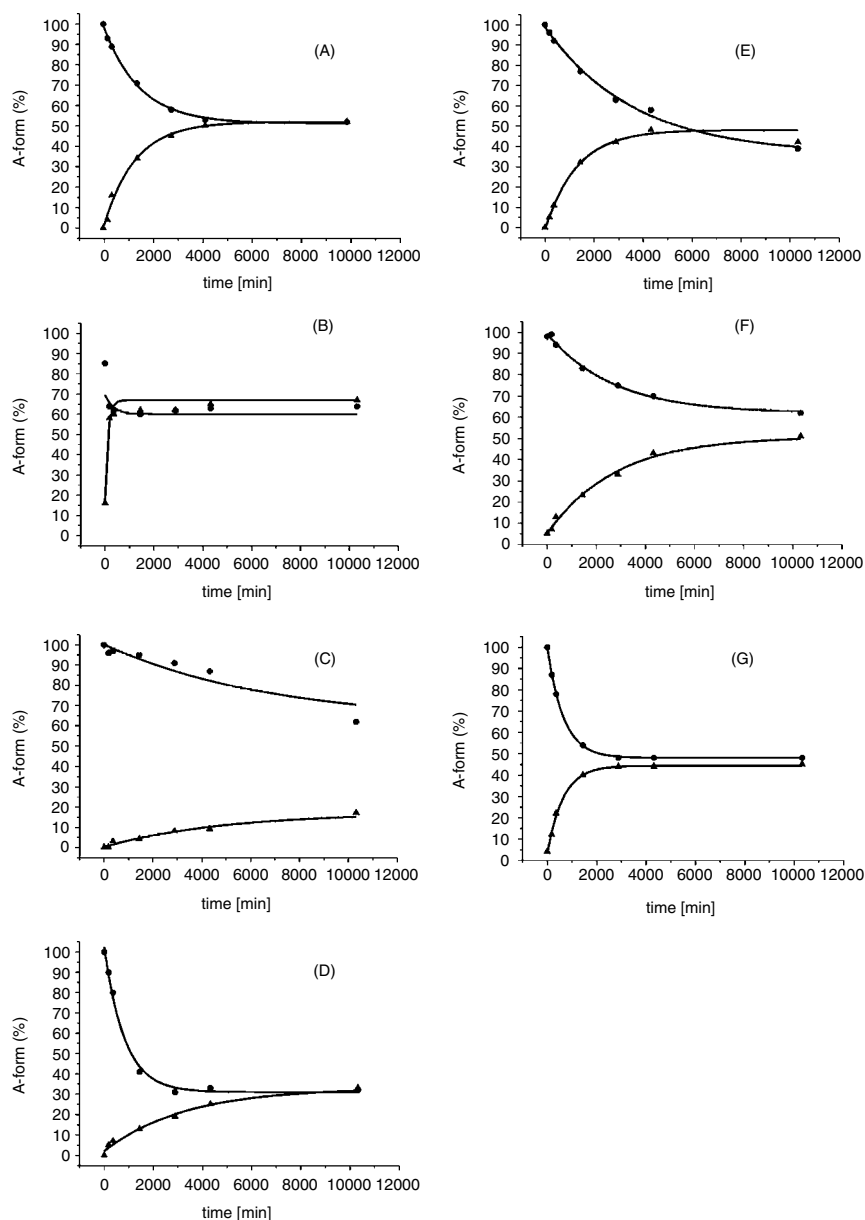


Figure 4 Interconversion kinetics of isoforms of selected uroguanylin derivatives. ● Interconversion of A-isoform; ▲ interconversion of B-isoform. Percentage of A-form after incubation at 37 °C is plotted against the incubation time and then analysed using a first order exponential fit function (GraphPad Prism, (for details see Materials and Methods). (A) uroguanylin-(1-16) **13**; (B) [Ala¹⁶]-uroguanylin-(1-16) **14**; (C) [Ala¹⁴]-uroguanylin-(1-16) **15**; (D) [Ala⁸]-uroguanylin-(1-16) **19**; (E) [Ala⁶]-uroguanylin-(1-16) **20**; (F) [Pro¹⁰]-uroguanylin-(1-16) **26**; (G) [Ala⁸, Tyr⁹, Ala¹⁰]-uroguanylin-(1-16) **25**.

faster than vice versa (Figure 4C). Exchanges of the amino acids adjacent to Cys⁷ (peptides **19** and **20**) led to different interconversion kinetics depending on the starting isoform. For peptide **19**, the equilibrium ratio of the isomers was 3:7, in which isomer B was more highly populated than isomer A, probably due to different thermodynamic stabilities of the isoforms (Figure 4D). The energy barrier for the interconversion from isomer B to A appeared to be higher than vice versa, resulting in a slower interconversion from isomer B to A. In contrast, the [Ala⁶]-uroguanylin A-isoform **20** transformed more slowly than the B-isoform (Figure 4E). The uroguanylin-ST hybrid peptide **26** (Figure 4F) exhibited a clearly slower conversion compared with native uroguanylin **13**, whereas the uroguanylin-guanylin hybrid **25** (Figure 4G) exhibited an increased interconversion rate. Substitution of the central Asn⁹ residue by Ala (peptide **18**) led to an accelerated interconversion (Table 2). This might be due to the lacking potential of Ala to form a side chain hydrogen bond. For some peptides, the interconversion rate was dependent on the starting isoform. For uroguanylin peptides **19**, **20**, **22** and **23**, one isomer showed a faster interconversion compared with native uroguanylin **13**, whereas the other isomer interconverted more slowly compared with peptide **13**. The L-Alanine substitutions that led to a significantly faster conversion from the A- to the B-form compared with native uroguanylin were those of the mutants Leu¹⁶ **14**, Asn⁹ **18**, Val⁸ **19**, Asp³ **22** and the exchange of [Val⁸, Asn⁹, Val¹⁰] to [Ala⁸, Tyr⁹, Ala¹⁰]-uroguanylin **25**. A slower interconversion rate from the A- to the B-isoform was observed for the mutants [Ala⁶]-uroguanylin **20** and [Pro¹⁰]-uroguanylin **26** as well as for peptides **21** and **23**. Amino acid replacements that led to a significantly faster conversion from the B- to the A-form were found for Leu¹⁶ **14**, Asn⁹ **18**, Asp² **23** and the triple mutant peptide **25**. A decreased interconversion rate from the B- to the A-isoform was detected for the derivatives [Ala⁸]-uroguanylin **19** and [Pro¹⁰]-uroguanylin **26** (Table 2). In summary, substitutions at the COOH-terminal part (residues 14 and 16) of uroguanylin have the greatest influence on the interconversion, while exchange of Gly¹⁴ to Ala slows down the interconversion. The opposite effect is observed, when Leu¹⁶ is replaced by Ala.

NMR-spectroscopic Analysis of Guanylin and Uroguanylin Peptides

In order to gain further insight into the structural properties of selected guanylin and uroguanylin derivatives, 2D NMR spectroscopy was performed with selected peptides exhibiting significantly different HPLC elution and interconversion characteristics to those of native guanylin and uroguanylin.

Guanylin Peptides

The guanylin peptides **2**, **4**, and **5** have been investigated by NMR spectroscopy (Table 3). In contrast to the uroguanylin peptides, the guanylin isomers could not be separated by chromatography, and the HPLC data suggested that the interconversion equilibrium was reached within 30 min. Therefore, only the investigation of a mixture of the two isomers was possible by NMR spectroscopy. As no exchange between the isomers of either of the peptides and also no line-broadening was observed, it is assumed that the isomers have a half-life of at least seconds. Complete sequence-specific resonance assignment was possible for all derivatives examined except for Pro¹ of peptides **4** and **5**. For native guanylin, chemical shift values are available for a 22-residue derivative [5]. However, those values were obtained at different temperatures and pH compared with our investigations. A guanylin derivative COOH-terminally extended by one leucine residue [Leu¹⁶]-guanylin-(1–15) was investigated earlier [7]. This derivative was analysed by NMR-spectroscopy under the same solution conditions as used for the alanine-substituted peptides of the present work. It was demonstrated that the COOH-terminal extension had no significant influence on the three-dimensional structures of the isomers [7]. Therefore, the chemical shift values obtained in the present work were compared with those of the COOH-terminally extended guanylin-Leu peptide and the deviations are given in Table 3. From this comparison, the chemical shift differences for the COOH-terminal cysteine residue were not meaningful due to the influence of endgroup effects and were therefore disregarded.

A substitution of Gly¹⁴ by Ala in peptide **2** caused no H α chemical shift deviation by more than 0.1 ppm for both isomers, except for Tyr⁹ of isomer B with a Δ ppm value of -0.11 . No deviations exceeding 0.2 ppm were found for the amide proton resonances of the two isomers. For isomer A only Tyr⁹ and Cys¹² and for isomer B the residues Tyr⁹, Ala¹⁰ and Ala¹¹ showed amide proton chemical shift deviations greater than 0.13 ppm, indicating that a substitution of Gly¹⁴ influences the central loop (see also uroguanylin peptide **15**).

The substitution of Tyr⁹ by Ala **4** had mainly a local influence on the backbone chemical shift values, most likely due to the loss of the aromatic system compared with native guanylin and with guanylin-Leu. The H α resonances of Ala⁸ preceding the substitution were significantly downfield-shifted (0.26 ppm for isomer A and 0.2 ppm for isomer B). All other H α resonances coincided with those of guanylin-Leu within a tolerance of 0.1 ppm, except for Thr¹³ of isomer A and Glu⁵ of isomer B. For the amide proton resonances, the largest deviations were found for Ala¹¹, Cys¹² and Gly¹⁴ of isomer A and Glu⁵ and Ala¹⁰ for isomer B, indicating that, except for the neighboring residues (Ala⁸, H α

Table 3 Chemical Shift Deviations (Δ ppm) of Guanylin-peptides **2**, **4** and **5** Compared with [Leu]¹⁶-guanylin-(1–15)^a

Residue	Δ ppm 2a		Δ ppm 2b		Δ ppm 4a		Δ ppm 4b		Δ ppm 5a		Δ ppm 5b	
	H α	HN	H α	HN	H α	HN	H α	HN	H α	HN	H α	HN
Pro ¹	0.05		0.01									
Gly ²	0.04	-0.09	0.03	0.04	0.08	-0.08	0.03	0.03	0.02	<u>-0.18</u>	0.04	0.05
Thr ³	-0.01	0.04	0.04	0.03	-0.05	0.08	0.03	0	0.06	0.05	0.06	0.03
Cys ⁴	0.01	-0.03	0	-0.03	-0.04	-0.06	0	0	<u>0.12</u>	0.09	0.06	0.09
Glu ⁵	-0.01	0.05	-0.03	<u>0.11</u>	-0.09	-0.06	<u>0.12</u>	<u>0.15</u>	-0.05	0.03	<u>-0.1</u>	0.01
Ile ⁶	-0.06	0.01	0.03	-0.01	-0.05	0.04	0.04	-0.01	—	—	—	—
Cys ⁷	0.02	0.03	0.02	-0.06	0.07	0.09	0.05	-0.02	<u>-0.15</u>	<u>-0.17</u>	<u>-0.2</u>	<u>-0.26</u>
Ala ⁸	0.07	0.06	-0.01	0.04	<u>0.26</u>	<u>0.11</u>	<u>0.2</u>	-0.03	-0.09	-0.01	0.09	-0.02
Tyr ⁹	-0.05	<u>0.19</u>	<u>-0.11</u>	<u>0.19</u>	—	—	—	—	<u>0.13</u>	<u>-0.35</u>	0.01	<u>0.13</u>
Ala ¹⁰	-0.07	0.06	0.05	<u>-0.14</u>	0.08	-0.01	-0.01	<u>0.14</u>	0.03	<u>0.13</u>	-0.03	<u>0.14</u>
Ala ¹¹	0.01	-0.01	<u>0.1</u>	<u>-0.18</u>	0.01	<u>0.18</u>	0.05	-0.01	0	<u>-0.13</u>	-0.01	0.03
Cys ¹²	0.05	<u>0.17</u>	0.08	0.01	0.07	<u>0.13</u>	0.05	0.05	-0.09	-0.07	0.07	-0.09
Thr ¹³	0.06	-0.04	0.02	0.08	<u>0.13</u>	-0.01	0.08	-0.01	0.05	-0.04	0.06	-0.07
Gly ¹⁴	—	—	—	—	0.06	<u>-0.13</u>	0.02	-0.05	0.02	<u>0.15</u>	0.04	0.07
Cys ¹⁵												

^a See reference [7] for details. The values obtained for [Leu]¹⁶-guanylin-(1–15) [7] were subtracted from the corresponding values of the mutant peptides. Therefore, an upfield-shift compared with the reference peptide [Leu]¹⁶-guanylin-(1–15) appears as a negative value in the table. Deviations ≥ 0.1 ppm are highlighted.

resonance and Ala¹⁰, amide proton resonance), the backbone chemical shifts of Glu⁵ of isomer B were slightly influenced. All other backbone chemical shifts of isomer B of peptide **4** coincided with those of guanylin-Leu within a tolerance of 0.1 ppm.

The substitution of Ile⁶ by Ala in peptide **5** appeared to have an influence on the central loop of both isomers and on both termini of isomer A. For both isomers, the H α resonance of Cys⁷ directly following the mutated sequence position was upfield-shifted by up to -0.2 ppm (isomer B), and a downfield shift was observed for Cys⁴ and Tyr⁹ of isomer A. All other deviations of the H α resonances of both isomers were less than 0.1 ppm. The amide proton chemical shift of Cys⁷ of isomer B was upfield-shifted by -0.26 ppm compared with guanylin-Leu and the amide proton resonances of Tyr⁹ and Ala¹⁰ were slightly downfield-shifted. The influence on the amide proton chemical shifts of isomer A were more pronounced. Not only the amide proton resonance of Cys⁷ directly following the substituted position was upfield-shifted, but also that of Gly², Tyr⁹ and Ala¹¹, while the amide proton resonance of Ala¹⁰ and Gly¹⁴ was downfield-shifted. An influence of the substitution on the backbone geometry of both isomers of peptide **5** cannot be excluded. Anyhow, exactly two isomers have been identified that showed backbone chemical shift values similar to the respective isomers of wild-type guanylin. Therefore, it is concluded that the general shape of the two isomers is still similar to native guanylin and only local distortions of the central loop geometry of both isomers of peptide **5** are assumed.

The range of the backbone proton deviations of the other two peptides **2** and **4** was much smaller, leading to the assumption that the corresponding alanine substitutions do not influence the backbone geometry of the isomers of these peptides. Therefore, the three-dimensional structures of the isomers of peptides **2** and **4** are most likely similar to those of native guanylin.

Uroguanylin Peptides

Based on the HPLC characteristics, uroguanylin peptides **14**, **15**, **19** and **26** were investigated by NMR spectroscopy at 11 °C and their backbone chemical shift values were compared with those of the corresponding isomers of wild-type uroguanylin **13** (Table 4) [6]. In all cases, the two isomers were separated by HPLC, allowing an NMR analysis of the single isoforms. Complete sequence-specific resonance assignment was possible for all isomers.

Comparison with the backbone chemical shifts of the respective isomers of native uroguanylin **13**, measured under identical conditions, revealed that the corresponding shifts of both isomers of peptide **14** differed by not more than 0.1 ppm. This indicated that the exchange of Leu¹⁶ for Ala only influenced the rate of interconversion but not the three-dimensional structure of both isomers of **14**.

For peptide **15**, the backbone geometry of both isoforms seemed to be influenced by the substitution of Gly¹⁴ by Ala. The H α chemical shifts of isomer A differed by less than 0.1 ppm from the corresponding shifts of native uroguanylin, except for Val⁸ with a slightly

Table 4 Chemical Shift Deviations (Δ ppm) of Uroguanylin-peptides **14**, **15**, **19**, and **26** Compared with Native Uroguanylin (peptide **13**)^a

Residue	Δ ppm 14a		Δ ppm 14b		Δ ppm 15a		Δ ppm 15b		Δ ppm 19a		Δ ppm 19b		Δ ppm 26a		Δ ppm 26b	
	H α	HN	H α	HN	H α	HN	H α	HN	H α	HN	H α	HN	H α	HN	H α	HN
Asn ¹	0.02		0.02		0.02		0.02		0.02		0.03		0.02		0.03	
Asp ²	-0.02	-0.03	-0.04	-0.04	-0.02	-0.02	-0.04	-0.04	-0.03	-0.02	0	-0.01	0	0	-0.02	0.01
Asp ³	-0.04	-0.03	-0.03	-0.06	-0.01	-0.02	0.02	-0.07	-0.02	-0.03	0	-0.04	0.01	0.01	-0.01	-0.01
Cys ⁴	0.06	0.08	-0.01	0.06	0.01	0.09	-0.01	0.01	0.04	0.08	0	0.06	0.08	0.04	0.01	0.02
Glu ⁵	-0.02	0.03	0.01	0.07	-0.02	0	0.01	0.07	0	0.08	0.03	<u>0.11</u>	0.01	0.03	0.01	0.09
Leu ⁶	0	<u>0.1</u>	0.03	-0.02	0.03	-0.03	0.03	0.02	0.05	0.07	0.03	-0.03	-0.05	<u>0.1</u>	0.03	-0.04
Cys ⁷	-0.03	-0.03	0.04	0.02	0	-0.05	0.09	0.03	<u>-0.12</u>	-0.04	-0.02	0.03	-0.08	-0.06	0.01	-0.02
Val ⁸	-0.04	-0.03	0.03	0.01	<u>0.12</u>	0.06	0.01	-0.04	—	—	—	—	-0.02	-0.01	0	<u>0.13</u>
Asn ⁹	0.03	-0.08	0.02	-0.02	-0.04	<u>0.21</u>	<u>-0.13</u>	<u>0.53</u>	0.07	<u>-0.27</u>	0.04	<u>-0.18</u>	0	-0.08	0.03	<u>-0.27</u>
Val ¹⁰	-0.02	0.02	-0.01	0.02	0.07	0.07	<u>0.14</u>	<u>-0.39</u>	0.02	<u>0.12</u>	0	0.1	—	—	—	—
Ala ¹¹	0.01	-0.02	0.01	0.03	0.01	0.08	0.05	-0.02	0.02	<u>0.11</u>	0.05	-0.02	-0.02	<u>-0.19</u>	0.03	-0.03
Cys ¹²	-0.03	-0.01	0	0.03	<u>0.1</u>	0.05	0.04	<u>0.22</u>	-0.01	0.04	0.03	-0.06	-0.03	0.09	0	0
Thr ¹³	0.01	0.04	0.08	-0.01	-0.05	-0.04	-0.07	<u>0.13</u>	0.03	0.02	0.03	<u>0.17</u>	0.05	-0.01	0.02	<u>-0.19</u>
Gly ¹⁴	-0.06	0.05	-0.01	0.02	—	—	—	—	-0.09	0.01	0.01	0.06	-0.09	-0.02	-0.03	<u>0.17</u>
Cys ¹⁵	0.03	0.01	0	0.04	0.02	<u>0.16</u>	0.02	<u>-0.15</u>	0.02	0.01	0.02	0.02	0	-0.01	0.01	<u>0.11</u>
Leu ¹⁶	—	—	—	—	-0.06	<u>-0.44</u>	-0.08	<u>-0.37</u>	-0.05	<u>-0.15</u>	-0.04	<u>-0.13</u>	0	-0.06	-0.05	<u>-0.12</u>

^a See reference [6] for details. The values obtained for wild-type uroguanylin [6] were subtracted from the corresponding values of the mutant peptides. Therefore, an upfield-shift compared with the reference peptide appears as a negative value in the table. Deviations ≥ 0.1 ppm are highlighted.

higher deviation. The amide proton shifts of isomer A were within the 0.1 ppm threshold, except for Asn⁹, Cys¹⁵ and Leu¹⁶. Amide proton chemical shifts appear to be highly sensitive to local sequence variations [27], providing an explanation for the shift deviations of Cys¹⁵ and Leu¹⁶ close to the substituted position. The amide proton of Asn⁹ was downfield-shifted by 0.21 ppm relative to native uroguanylin. Together with the H α chemical shift deviation of Val⁸, this indicated an influence of the substitution on the central loop of isomer A of peptide **15**. For the corresponding B isomer, the same regions were affected by the substitution: the H α chemical shifts of Asn⁹ and Val¹⁰ differed by -0.13 and 0.14 ppm from those of wild-type uroguanylin. All other H α shift deviations were within 0.1 ppm. The amide proton chemical shifts of the residues flanking the substitution (Cys¹², Thr¹³, Cys¹⁵ and Leu¹⁶) showed deviations of more than 0.1 ppm. More interestingly, residues Asn⁹ and Val¹⁰ of the central loop of isomer B of peptide **15** were significantly affected with amide proton chemical shift deviations of 0.53 and -0.39 ppm.

The exchange of Val⁸ for Ala in peptide **19** had only minor effects on the backbone chemical shifts of the two isomers. The deviations of the H α proton resonances of both isomers were within the threshold of 0.1 ppm, except for Cys⁷ (preceding the substituted position) of isomer A with a slightly increased chemical shift deviation from wild-type uroguanylin. For the amide proton resonances, that of Asn⁹ (following the substituted position) exhibited the largest deviation:

-0.27 ppm for isomer A and -0.18 ppm for isomer B. All other deviations were within 0.17 ppm (highest deviation found for Thr¹³ of isomer B) with altogether only four differences of each isomer exceeding 0.1 ppm.

The exchange of Val¹⁰ for Pro in **26** led to a peptide that is considered a hybrid between uroguanylin and *E. coli* heat-stable enterotoxin ST (for ST sequence see Figure 1). For both isomers, the Asn-Pro peptide bond exhibited *trans* conformation as found for the crystal structure of ST [28]. It is well known that the H α chemical shift of a residue preceding a proline is significantly downfield-shifted and correction values have been suggested [29]. Taking such a correction into account, all H α chemical shifts of both isomers of peptide **26** were similar to those of native uroguanylin within a tolerance of 0.1 ppm. The amide proton resonances of isomer A differed by less than 0.1 ppm from those of native uroguanylin, except for Ala¹¹ directly following the substituted position (Δ ppm: -0.19). The effect on the amide proton chemical shifts of isomer B was somewhat greater. Besides the preceding residues Asn⁹ (-0.27 ppm) and Val⁸ (0.13 ppm), residues Thr¹³, Gly¹⁴ and Cys¹⁵ exhibited deviations by more than 0.1 ppm (up to -0.19 ppm for Thr¹³).

In summary, the chemical shift deviations between the isomers of the investigated uroguanylin-derived peptides and the corresponding isomers of native uroguanylin were quite similar, indicating that the isomers exhibit structures similar to those of native

uroguanylin. Thus, the substitutions do not drastically affect the three-dimensional structures of the uroguanylin isomers. From these results it is concluded that the uroguanylin derivatives exhibit conformational properties similar to those of the related isoforms of native uroguanylin. Explicit structure calculations for the various isomers were therefore not necessary.

Substitutions within the central loop of native uroguanylin (peptides **19** and **26**) appear to have a slight influence on the chemical shifts of residues between the last two cysteines, especially for the B isomers. The substitution of Gly¹⁴ for alanine (peptide **15**) influences backbone chemical shifts of the central loop (see also guanylin peptide **2**). Furthermore, the comparison of chemical shifts revealed that, for all peptides investigated, the earlier eluting isomer (isomer A) is indeed the isoform that structurally resembles *E. coli* ST.

For all derivatives of guanylin and uroguanylin investigated by NMR spectroscopy, two defined isomers have been identified that show backbone chemical shift values similar to the respective isomers of the native peptides. Therefore, it is concluded that the three-dimensional structures of the isomers are highly similar to those of the native peptides.

DISCUSSION

To our knowledge, guanylin and uroguanylin are the only mammalian peptides that have been demonstrated to exist as topological isomers [4–9]. Little is published about members of the conotoxin family, membrane channel-inhibitory peptides produced by *Conus* snails living in tropical waters which may exhibit similar characteristics. Conotoxin MI has been shown to exhibit two different conformational states at chromatographic conditions similar to those used for guanylin isomers [30]. Isoforms of different α -conotoxins containing a disulfide pattern similar to that of guanylin-like peptides have also been analysed using NMR spectroscopy, but nothing is known about the interconversion of these peptides [17]. These peptides, however, contain a proline or hydroxyproline residue that gives rise to *cis/trans* isomerism.

The present study focuses on side chain contributions to the interconversion of guanylin and uroguanylin isomers which do not contain proline or hydroxyproline residues. Understanding of the present topological isomerism that is due solely to a certain defined disulfide pattern and of the associated mechanism of interconversion is of general interest and may also be valuable for understanding the structural characteristics of other peptides with two or more disulfide bonds. In addition, the pharmacologic potential of the peptide hormones guanylin and uroguanylin with

respect to the development of GC-C agonists and antagonists requires the understanding and control of the mechanism underlying the isomerism.

There are three different hypothetical possibilities for a sterically controlled interconversion between the two isoforms (Figure 5) [6,31]. The schematic structures of the A- and B-isomers suggest that an interconversion may occur by (A) threading the loop between the inner cysteines through the ring formed by the two disulfide bonds and the amino acids between these cysteines (Figure 5A), (B) threading the NH₂-terminus through the ring built by the backbone of the residues Cys⁷ to Cys¹⁵ and the disulfide bridge between Cys⁷ and Cys¹⁵ (Figure 5B), and (C) threading the COOH-terminus through the ring formed by the peptide backbone from Cys⁴ to Cys¹² and the disulfide bond between Cys⁴ and Cys¹² (Figure 5C).

Pathway (A) can be excluded by interconversion experiments using synthetic guanylin peptides which contain a significant sterical hindrance in the loop. Neither substitution of the central segment AYA by VNV (peptide **11**) nor by the less hindering AGG sequence significantly influences the interconversion kinetics of the two isoforms of 15- and 17-residue guanylin peptides as reported earlier [4]. In addition, the introduction of a bulky diiodotyrosine at position Tyr⁹ has virtually no effect on the isomerization kinetics of guanylin [7]. Pathway (B) can be excluded because the mutual interconversion of the native uroguanylin isomers (peptide **13**) and those of a NH₂-terminally longer uroguanylin consisting of 24 residues exhibit kinetically identical characteristics, as determined by HPLC analysis earlier [6]. Further synthetic derivatives of guanylin and uroguanylin proved an interconversion following pathway (C) [7,8]. Uroguanylin lacking Leu¹⁶ does not form two separable isomers. This peptide shows a guanylin-like chromatographic behavior, i.e. two observable but inseparable HPLC peaks at low temperature [8]. Moreover, a guanylin derivative extended by a COOH-terminal leucine was synthesized and examined yielding two separable isomers whose stability resembles that of uroguanylin isomers [7]. Thus, it has been suggested that the interconversion rate of the conformational exchange of guanylin-like peptides is under the sterical control of COOH-terminal residues [6,7,31].

The present systematic study with L-alanine scan peptides and chimeras of guanylin, uroguanylin and ST peptides corroborates and refines the proposed interconversion mechanism. Among the synthetic L-alanine guanylin derivatives, the Gly¹⁴ substitution of peptide **2** was the only exchange causing a stabilization of the isomers. For the corresponding uroguanylin derivative **15**, an enhanced kinetic stability of both isomers was observed. This can simply be explained by a higher energy barrier for the conversion induced by the steric hindrance of the additional methyl

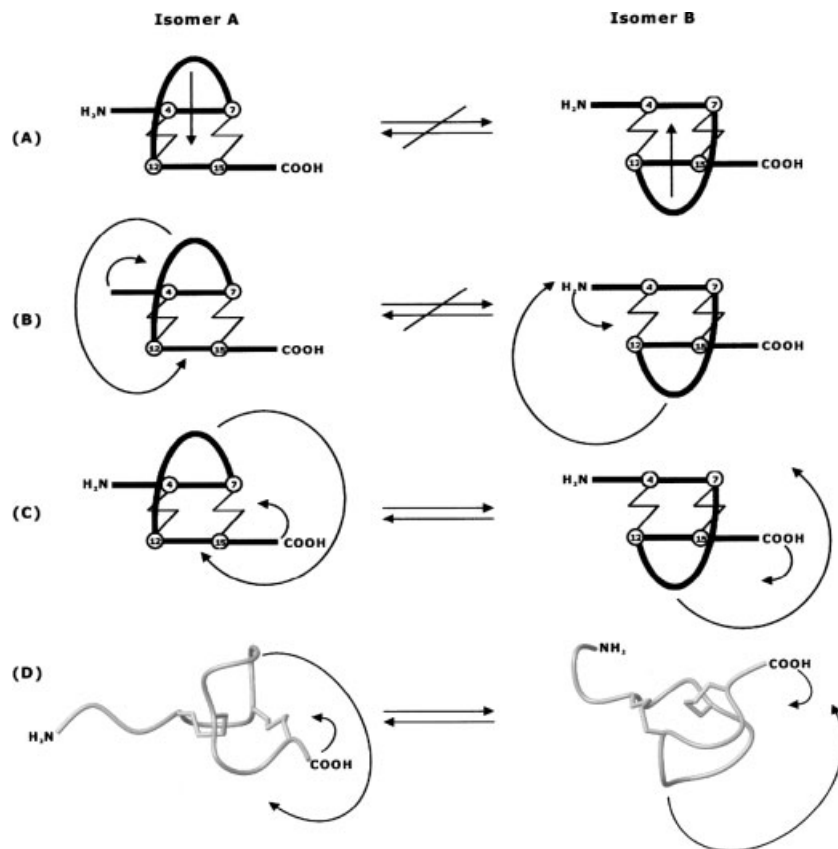


Figure 5 Schematic mechanism of interconversion of guanylin and uroguanylin isomers. (A) Pathway A: the loop is threaded through the ring formed by the two disulfide bonds; (B) pathway B: the NH_2 -terminus is threaded through the ring formed by the backbone and the disulfide bridge between Cys⁴ and Cys¹²; (C) pathway C: the COOH-terminus is threaded through the ring built by the backbone and the disulfide bridge between Cys⁷ and Cys¹⁵; (D) proposed mechanism of interconversion of guanylin/uroguanylin peptides represented by the structures of uroguanylin isoforms [6]. Molscript models are based on entries 1UGA and 1UGB deposited in the Brookhaven Protein Data Bank. Arrows indicate the movement of the molecule.

group at position 14 of guanylin and uroguanylin. All other guanylin mutations led either to an increased isomerization rate or the isoforms were not detectable by HPLC. The double mutant [Asn⁹, Pro¹⁰]-guanylin **12** confirms that sterical changes in the central loop between the inner cysteines do not significantly alter the characteristics of the interconversion.

For the isomers of native uroguanylin, the interconversion occurs with the supply of thermal energy. A COOH-terminal elongation thus has the strongest impact on the stabilization of the isomers. This is due to the sterical effect of the branched leucine side chain at the COOH-terminus, since the mutation of the terminal leucine to a smaller alanine residue (peptide **14**) results in an increase of the interconversion rate. In accordance with the corresponding guanylin mutation (peptide **2**), [Ala¹⁴]-uroguanylin **15** exhibits a significant decrease of the interconversion rate of both isomers. These results confirm that the interconversion route is in accordance with pathway (C) (Figure 5C). Mutations in the central and NH_2 -terminal part of uroguanylin influence the interconversion only to a minor extent. Mainly, the introduction of sterically less hindered residues in the

central loop segment of **18** and **25** led to an acceleration of interconversion. This is in accordance with our proposed model for interconversion (Figure 5C) since higher flexibility of the central loop would facilitate an interconversion according to pathway (C). The introduction of a more rigid proline residue into the central loop (peptide **26**) leads to a slower interconversion.

Furthermore, some alanine substitutions exert influence on the ratio of the two isomers which is associated with different transformation rates depending on the starting isoform (for example **19**, **20**, **22**, **23**), probably due to different thermodynamic stabilities of the two isomers resulting in different energy barriers for the mutual interconversion. In the case of peptides **19** and **20**, the differences in the thermodynamic stability of the A- and B-isomers are most likely due to sterical reasons since neutral residues are substituted by alanine. In the case of peptides **22** and **23**, electrostatic or hydrogen bondings may be involved as the NH_2 -terminal residues do not directly participate in the interconversion. Electrostatic or hydrogen bondings are assumed between Asn⁹ and Asp³ for isomer A of native uroguanylin and between Asn⁹ and Asp² for isomer B.

This assumption is based on the interconversion behavior of peptides **22** and **23** as a substitution of Asp³ by Ala (peptide **22**) led to an accelerated interconversion from A to B and a substitution of Asp² **23** caused a faster interconversion from B to A. Such interactions provide an additional explanation for the accelerated interconversion of both isomers of peptide **18**. These interactions, however, are not directly observable by ¹H NMR spectroscopic analysis of native uroguanylin [6], but are likely, at least for isomer A, since side chain interactions between the residues at positions 3 and 9 are very close to the position of the third disulfide bond of ST (Figure 1).

In summary, the interconversion of the isomers of guanylin and uroguanylin is a dynamic process that is influenced by several factors: the sterical hindrance caused by the COOH-terminal residues which have the strongest influence (peptides **2**, **14**, **15**), the potential hydrogen bonding between residues of the NH₂-terminus and residues of the central loop with moderate impact (peptides **7**, **18**, **22**, **23**), and by the flexibility within the loop region also with moderate influence (peptides **11**, **12**, **25**, **26**) (Figure 5D). These results demonstrate that kinetic control of the interconversion process is possible by the selective introduction of suitable side chains at various sequence positions. This control is important for the development of peptide agonists and antagonists of GC-C. Furthermore, the backbone and disulfide connectivity of guanylin-like peptides may serve as a molecular template that allows a defined switch between two distinct molecular conformations.

Acknowledgements

U.C.M. gratefully acknowledges support of the Deutsche Forschungsgemeinschaft (MA2317-1) and the Bayerischer Habilitationsförderpreis.

REFERENCES

- Currie MG, Fok KF, Kato J, Moore RJ, Hamra FK, Duffin KL, Smith CE. Guanylin: an endogenous activator of intestinal guanylate cyclase. *Proc. Natl Acad. Sci. USA* 1992; **89**: 947–951.
- Wiegand RC, Kato J, Huang MD, Fok KF, Kachur JF, Currie MG. Human guanylin: cDNA isolation, structure, and activity. *FEBS Lett.* 1992; **311**: 150–154.
- Hamra FK, Forte LR, Eber SL, Pidhorodeckyj NV, Krause WJ, Freeman RH, Chin DT, Tompkins JA, Fok KF, Smith CE, Duffin KL, Siegel NR, Currie MG. Uroguanylin: structure and activity of a second endogenous peptide that stimulates intestinal guanylate cyclase. *Proc. Natl Acad. Sci. USA* 1993; **90**: 10464–10468.
- Klodt J, Kuhn M, Marx UC, Martin S, Rösch P, Forssmann WG, Adermann K. Synthesis, biological activity and isomerism of guanylate cyclase C-activating peptides guanylin and uroguanylin. *J. Pept. Res.* 1997; **50**: 222–230.
- Skelton NJ, Garcia KC, Goeddel DV, Quan C, Burnier JP. Determination of the solution structure of the peptide hormone guanylin: observation of a novel form of topological stereoisomerism. *Biochemistry* 1994; **33**: 13581–13592.
- Marx UC, Klodt J, Meyer M, Gerlach H, Rösch P, Forssmann WG, Adermann K. One peptide, two topologies: structure and interconversion dynamics of human uroguanylin isomers. *J. Pept. Res.* 1998; **52**: 229–240.
- Schulz A, Escher S, Marx UC, Meyer M, Rösch P, Forssmann WG, Adermann K. Carboxy-terminal extension stabilizes the topological stereoisomers of guanylin. *J. Pept. Res.* 1998; **52**: 518–525.
- Chino N, Kubo S, Miyazato M, Nakazato M, Kangawa K, Sakakibara S. Generation of two isomers with the same disulfide connectivity during disulfide bond formation of human uroguanylin. *lett. Pept. Sci.* 1996; **3**: 45–52.
- Chino N, Kubo S, Kitani T, Yoshida T, Tanabe R, Kobayashi Y, Nakazato M, Kangawa K, Kimura T. Topological isomers of human uroguanylin: interconversion between biologically active and inactive isomers. *FEBS Lett.* 1998; **421**: 27–31.
- Carpick BW, Garipey J. The *Escherichia coli* heat-stable enterotoxin is a long-lived superagonist of guanylin. *Infect. Immun.* 1993; **61**: 4710–4715.
- Garipey J, Lane A, Frayman F, Wilbur D, Robien W, Schoolnik GK, Jardtzyk O. Structure of the toxic domain of the *Escherichia coli* heat-stable enterotoxin ST I. *Biochemistry* 1986; **25**: 7854–7866.
- Field M, Semrad CE. Toxicogenic diarrheas, congenital diarrheas, and cystic fibrosis: disorders of intestinal ion transport. *Annu. Rev. Physiol.* 1993; **55**: 631–655.
- Farthing MJ. Travellers' diarrhoea. *Gut* 1994; **35**: 1–4.
- Orndorff GR, Sadjimin T, Simanjuntak CH, O'Hanley P, Punjabi NH, Tjokrosonto S, Corwin A, Dibley M, Lebron CI, Echeverria P. Enterotoxigenic *Escherichia coli* diarrhea in children less than five years of age in central Java. *Am. J. Trop. Med. Hyg.* 1996; **55**: 449–451.
- Lorenz JN, Nieman M, Sabo J, Sanford LP, Hawkins JA, Elitsur N, Gawenis LR, Clarke LL, Cohen MB. Uroguanylin knockout mice have increased blood pressure and impaired natriuretic response to enteral NaCl load. *J. Clin. Invest.* 2003; **112**: 1244–1254.
- Shailubhai K, Yu HH, Karunanandaa K, Wang JY, Eber SL, Wang Y, Joo NS, Kim HD, Miedema BW, Abbas SZ, Boddupalli SS, Currie MG, Forte LR. Uroguanylin treatment suppresses polyp formation in the Apc^{Min/+} mouse and induces apoptosis in human colon adenocarcinoma cells via cyclic GMP. *Cancer Res.* 2000; **60**: 5151–5157.
- Favreau P, Krimm I, Le Gall F, Bobenrieth MJ, Lamthanh H, Bouet F, Servent D, Molgo J, Menez A, Letourneux Y, Lancelin JM. Biochemical characterization and nuclear magnetic resonance structure of novel alpha-conotoxins isolated from the venom of *Conus* consors. *Biochemistry* 1999; **38**: 6317–6326.
- Gouda H, Yamazaki K, Hasegawa J, Kobayashi Y, Nishiuchi Y, Sakakibara S, Hirono S. Solution structure of alpha-conotoxin MI determined by ¹H-NMR spectroscopy and molecular dynamics simulation with the explicit solvent water. *Biochim. Biophys. Acta* 1997; **1343**: 327–334.
- Nielsen KJ, Watson M, Adams DJ, Hammarstrom AK, Gage PW, Hill JM, Craik DJ, Thomas L, Adams D, Alewood PF, Lewis RJ. Solution structure of μ -conotoxin PIIIA, a preferential inhibitor of persistent tetrodotoxin-sensitive sodium channels. *J. Biol. Chem.* 2002; **277**: 27247–27255.
- Jacobsen RB, Jimenez EC, De la Cruz RGC, Gray WR, Cruz LJ, Olivera BM. A novel D-leucine-containing *Conus* peptide: diverse conformational dynamics in the contryphan family. *J. Pept. Res.* 1999; **54**: 93–99.
- Jacobsen R, Jimenez EC, Grilley M, Watkins M, Hillyard D, Cruz LJ, Olivera BM. The contryphan family of *Conus* peptides: interconversion between conformers. *J. Pept. Res.* 1998; **51**: 173–179.
- Pallaghy PK, Melnikova AP, Jimenez EC, Olivera BM, Norton RS. Solution structure of contryphan-R, a naturally occurring disulfide-bridged octapeptide containing D-tryptophan: comparison with protein loops. *Biochemistry* 1999; **38**: 11553–11559.

23. Pallaghy PK, He W, Jimenez EC, Olivera BM, Norton RS. Structures of the contryphan family of cyclic peptides. Role of electrostatic interactions in cis-trans isomerism. *Biochemistry* 2000; **39**: 12 845–12 852.
24. Hwang TL, Shaka AJ. Water suppression that works. Excitation sculpting using arbitrary wave forms and pulsed field gradients. *J. Magn. Reson.* 1995; **112**: 275–279.
25. Cavannagh J, Rance M. Suppression of cross-relaxation effects on TOCSY spectra via a modified DIPSI-2 mixing sequence. *J. Magn. Reson.* 1992; **96**: 670–678.
26. Friedrich MS. A model-free algorithm for the removal of baseline artifacts. *J. Biomol. NMR* 1995; **5**: 147–153.
27. Merutka G, Dyson HJ, Wright PE. 'Random coil' ^1H chemical shifts obtained as a function of temperature and trifluoroethanol concentration for the peptide series GGXGG. *J. Biomol. NMR* 1995; **5**: 14–24.
28. Ozaki H, Sato T, Kubota H, Hata Y, Katsube Y, Shimonishi Y. Molecular structure of the toxin domain of heat-stable enterotoxin produced by a pathogenic strain of *Escherichia coli*. A putative binding site for a binding protein on rat intestinal epithelial cell membranes. *J. Biol. Chem.* 1991; **266**: 5934–5941.
29. Wishart DS, Bigam CG, Holm A, Hodges RS, Sykes BD. ^1H , ^{13}C and ^{15}N random coil NMR chemical shifts of the common amino acids. I. Investigations of nearest-neighbor effects. *J. Biomol. NMR* 1995; **5**: 67–81.
30. Gray WR, Rivier JE, Galyean R, Cruz LJ, Olivera MM. Conotoxin MI. Disulfide bonding and conformational states. *J. Biol. Chem.* 1983; **258**: 12 247–12 251.
31. Marx UC, Adermann K, Schulz A, Meyer M, Forssmann WG, Rösch P. Structure and function of biological macromolecules. In *Dynamics 2001*, Jardetzky O, Finucane MD (eds). IOS Press: Amsterdam, 2001; 145–161.